Applied Catalysis B: Environmental 150–151 (2014) 101–106

Contents lists available at ScienceDirect

Applied Catalysis B: Environmental

journal homepage: www.elsevier.com/locate/apcatb

Highly dispersed Pt/C catalysts prepared by the Charge Enhanced Dry Impregnation method

Chongjiang Cao[a,b], Guang Yang[c], Laetitia Dubau[d], Frédéric Maillard[d], Stéphanie D. Lambert[a], Jean-Paul Pirard[a], Nathalie Job[a,*]

[a] Laboratory of Chemical Engineering, Department of Applied Chemistry, University of Liège (B6a), B-4000 Liège, Belgium
[b] College of Food Science and Engineering, Nanjing University of Finance and Economics, Nanjing 210046, China
[c] Electronic Materials Research Laboratory, Key Laboratory of the Ministry of Education & International Center for Dielectric Research, Xi'an Jiaotong University, Xi'an 710049, China
[d] Laboratoire d'Électrochimie et de Physico-chimie des Matériaux et des Interfaces (LEPMI), UMR 5279 CNRS/Grenoble-INP/Université de Savoie/Université Joseph Fourier, BP75, F-38402 St Martin d'Hères Cedex, France

ARTICLE INFO

Article history:
Received 20 September 2013
Received in revised form
28 November 2013
Accepted 2 December 2013
Available online 8 December 2013

Keywords:
Platinum nanoparticles
Carbon xerogels
PEM fuel cells
Electrocatalyst

ABSTRACT

An efficient method to synthesize highly dispersed Pt/carbon xerogel catalysts for Proton Exchange Membrane fuel cell applications is described. The synthesis proceeds *via* the Charge Enhanced Dry Impregnation method (CEDI), which combines dry impregnation with the Strong Electrostatic Adsorption technique (SEA). The samples prepared *via* CEDI or SEA techniques were dried and reduced under hydrogen to obtain supported Pt nanoparticles. In order to increase the Pt mass fraction up to 10 wt.%, two successive impregnation-drying-reduction cycles were performed. The synthesized Pt nanoparticles are homogeneously distributed on the carbon support and highly dispersed (mean Pt nanoparticle size of *ca.* 2 nm). The CEDI method is ideally suited to avoid Pt losses during the catalyst preparation.

1. Introduction

Fuel cells are an attractive option for power generation, because of their high efficiency with little or no pollution [1,2]. Pt nanoparticles supported on a high surface area carbon support are commonly used in low temperature proton-exchange membrane fuel cells (PEMFCs) to catalyze the electrooxidation of H_2 (HOR) or small organics molecules at the anode and the electroreduction of O_2 (ORR) at the cathode [3]. The HOR is fast, thus allowing small Pt loadings to be used at the anode [4]. However, due to the sluggish oxygen reduction kinetics, high Pt loading is required at the cathode. In addition, both electrodes should be as thin as possible to minimize mass transport limitations, therefore requiring Pt/C electrocatalysts with high Pt mass fraction.

To decrease the mass of Pt used in the PEMFC electrodes, significant efforts have been devoted to improve the structure of both the electrocatalyst and the electrode. Firstly, since PEMFC reactions are structure-sensitive, optimal sizes of Pt nanoparticles exist for each reaction, *e.g.* ~3 nm sized Pt particles are the most active catalyst for the ORR per mass unit of platinum [5]. Generally speaking, the size of the Pt nanoparticles strongly affects the number and the turnover frequency of the catalytic sites, and therefore determines the overall catalyst performance [6–9]. Secondly, mass transport limitations, and thus the resulting loss of PEMFC efficiency, can be decreased by using carbon supports with appropriate pore texture. In that respect, nanostructured carbons [10], such as carbon xerogels [11–13], are interesting alternatives to carbon blacks. Indeed, carbon xerogels feature high purity and tailorable pore texture, which allows for better mass transport in the electrode [11]. Finally, the distribution of the electron and the ion conductors (Pt/C and Nafion®) is linked to the electrode processing: the manufacture method must then be optimized for each material used.

Previous works from our group reported the preparation of highly dispersed Pt/carbon xerogel electrocatalysts with high Pt mass fraction (10–25 wt.%) using the Strong Electrostatic Adsorption (SEA) method [13,14]. The SEA technique [15,16] consists in maximizing the electrostatic interactions between the metal precursor and the support by adjusting the pH of the carbon/water/Pt precursor slurry to the adequate value. The latter depends on the surface chemistry (and of the Point of Zero Charge, PZC) of the support and on the nature of the Pt precursor. Due to the presence of various chemical surface groups, the carbon support protonates/deprotonates at low/high pH value, thus enhancing the adsorption of anions/cations, respectively. For instance, in the case

* Corresponding author. Tel.: +32 4 366 3537; fax: +32 4 366 3545.
E-mail address: Nathalie.Job@ulg.ac.be (N. Job).

0926-3373/$ – see front matter © 2013 Elsevier B.V. All rights reserved.
http://dx.doi.org/10.1016/j.apcatb.2013.12.004

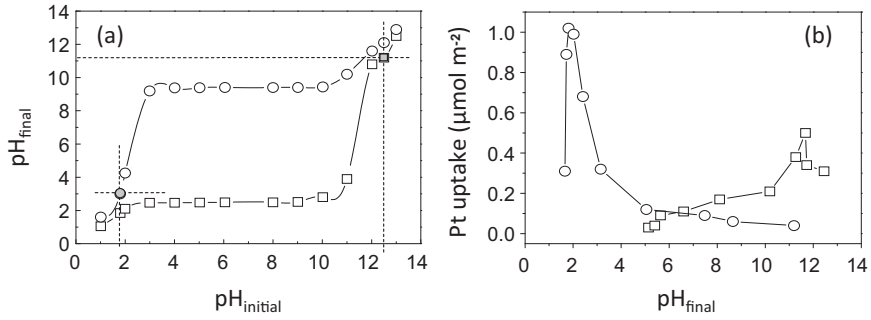

Fig. 1. (a) pH equilibrium for carbon supports at maximum surface loading: (○) raw carbon xerogel and (□) oxidized carbon xerogel and (b) Final metal precursor uptake *vs.* pH: (○) CPA on raw carbon xerogel (SL = 1000 $m^2\ L^{-1}$, 1000 ppm_{Pt} solution) and (□) PTA on oxidized carbon xerogel (SL = 1000 $m^2\ L^{-1}$, 200 ppm_{Pt} solution).

of the impregnation of carbon xerogels with chloroplatinic acid (CPA, H_2PtCl_6) aqueous solutions (1000 ppm_{Pt}), the final pH leading to the highest Pt uptake was found to be ~2.5, yielding electrocatalysts with Pt mass fraction close to 10 wt.% [14]. However, SEA-type impregnations were up to now performed in large excess of Pt precursor solution, resulting into drastic metal losses.

To minimize such losses, Zhu et al. [17] recently combined the SEA method with the classical dry impregnation technique. They synthesized 2 wt.% Pt catalysts supported on oxidized active carbon or gamma-alumina by this new technique, called the Charge Enhanced Dry Impregnation (CEDI) method. The optimal impregnation pH was first determined, then dry impregnation was performed using a Pt precursor solution ($[Pt(NH_3)_4]Cl_2$ or Na_2PtCl_4) whose pH was adjusted to the optimal impregnation value. The synthesized Pt nanoparticles were 2–3 nm in size, but the Pt mass fraction remained far too low for PEMFC applications. The aim of the present work is thus to show that the SEA method can be combined with the classical dry impregnation technique to prepare Pt/carbon xerogel catalysts with higher Pt mass fraction and high dispersion while avoiding any precursor loss. In this ambit, a carbon xerogel with chosen pore texture, raw or oxidized, was impregnated with appropriate Pt precursor solutions using the CEDI method to reach the highest Pt mass fraction in one run. In some cases, a second run was performed to check for the possibility of increasing the Pt mass fraction without altering the dispersion. The catalysts were then characterized using physico-chemical and electrochemical techniques.

2. Experimental

2.1. Synthesis of the carbon support

The chosen carbon support, named 'CX' hereafter, was a micro-macroporous carbon xerogel with a macropore size ranging from 50 to 85 nm and a specific surface area of 624 $m^2\ g^{-1}$, prepared following a method described elsewhere [18]. The carbon xerogel was obtained by evaporative drying and condensation of a resorcinol-formaldehyde aqueous gel. The gel was first prepared by polycondensation of resorcinol with formaldehyde in water, in the presence of Na_2CO_3. 9.91 g of resorcinol (Vel, 99%) and 0.00955 g of Na_2CO_3 (UCB, 99.5%) were dissolved into 18.8 mL of deionized water. After complete dissolution, 13.5 mL of formaldehyde (Aldrich 37 wt.% in water, stabilized with 10–15 wt.% methanol) were added. The resorcinol/formaldehyde molar ratio, *R*/*F*, was fixed at 0.5, which is usually considered as the stoichiometric ratio. The resorcinol/sodium carbonate molar ratio, *R*/*C*, was equal to 1000, while the solvents/(resorcinol + formaldehyde) molar ratio, *D* was chosen equal to 5.7. In *D*, the term 'solvent' includes the deionized water added, and the water and methanol (stabilizer) present in the formaldehyde solution. Gelation and aging were performed at 358 K for 72 h. The wet material was dried at 333 K in a vacuum oven by gradually decreasing the pressure down to 10^3 Pa over two days. The sample was then left at 423 K and 10^3 Pa for 12 h. Finally, the dry carbon xerogel was pyrolyzed under flowing nitrogen at 1073 K for 2 h.

The PZC of this carbon material was measured following the method described in Ref. [14]: briefly, the porous solid was soaked in water solution of various initial pH and, after stabilization, the pH was measured again. The PZC of the solid corresponds to a plateau in a plot of the final pH *vs.* the initial pH. For all measurements, the surface loading (SL), *i.e.* the total carbon surface in solution, was fixed at 1000 $m^2\ L^{-1}$. Fig. 1a shows that the PZC of the carbon xerogel equals 9.4.

In order to obtain a low PZC carbon support for catalyst preparation from Pt cations, the pristine carbon xerogel was oxidized by immersion in HNO_3 (5 N) during 48 h at room temperature, water washed and heated in helium at 473 K for 1 h to remove the most unstable functions. This support is labeled 'OX', and its PZC was measured equal to 2.4 following the same method as that used for the non-oxidized support (Fig. 1a).

2.2. Catalyst preparation

Fig. 2, shows that at pH lower than 9.4, the pristine carbon xerogel, CX, charges positively and adsorbs preferentially anions (*e.g.* $PtCl_6^{2-}$). On the contrary, at pH higher than 2.4, the adsorption of cations like *e.g.* platinum tetraamine ($[Pt(NH_3)_4]^{2+}$, PTA) is enhanced on OX due to the negative charge of the carbon surface. Following previous results obtained with the SEA technique, and because of repulsive effects when the pH becomes too low (adsorption of anions) or too high (adsorption of cations), an optimum pH leading to maximum metal mass fraction exists [13–16]. For instance, this optimal final pH is equal to ~2.5 for adsorption of H_2PtCl_6 (CPA) on CX [14], the maximum Pt mass fraction being found equal to 8–10 wt.% (note that the initial pH of the solution was 1.8). In the ambit of the present study, the optimal final pH of adsorption of PTA was determined following the same method, and was found equal to 11.2 (initial pH = 12.5), with a Pt uptake of 0.5 μmol m^{-2} (Fig. 1b), which corresponds to a Pt mass fraction of ~5 wt.%.

These results were then combined with the principles of the dry impregnation within the frame of the CEDI method. In a typical synthesis, the desired mass of metal coordination complex (CPA or PTA), corresponding to the maximum metal uptake first determined by the SEA method, was dissolved in a volume of deionized water corresponding to the amount necessary to wet the solid; this volume was determined by dropping deionized water (50 μL at a time) on the carbon support until it was just wet. The initial pH of the Pt precursor solution was then chosen according to the optimal final pH of the support/complex pair determined by SEA [14].

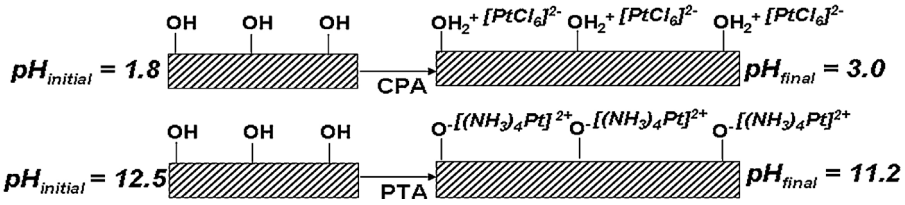

Fig. 2. Principles of enhancement of the electrostatic interactions between the carbon support and the Pt precursor.

Therefore, the initial pH was chosen as 1.8 and 12.5 for CPA/CX or PTA/OX adsorption, respectively. The samples were then directly dried in air at 298 K for 48 h and reduced in H_2 flow at 523 K for 1 h.

Several catalysts with Pt mass fractions equal to 5 or 10 wt.% were prepared either from CX as support and CPA as precursor, or using the OX-PTA pair. To achieve 10 wt.% of Pt with the CX-CPA pair, 0.23 g of CPA were dissolved in 3 mL deionized water, and the initial pH was adjusted to 1.8 with dilute HNO_3; this precursor solution was slowly added, 50 μL at a time, to 1 g of CX. The final pH, equal to 3.0, was measured by contacting the wet support with the pH-meter electrode. The sample was then dried in air at room temperature for 48 h, and reduced at 523 K in H_2 flow for 1 h. In the case of the OX-PTA pair, and for a targeted 5 wt.% Pt/OX, the precursor solution was prepared by dissolving 0.1 g PTA nitrate ($[Pt(NH_3)_4](NO_3)_2$) in 3 mL deionized water; the pH was adjusted to 12.5 with NH_4OH. Again, 1 g of support (OX) was contacted with the precursor solution by adding the latter 50 μL at a time to the carbon powder. The final pH was measured equal to 11.2.

In order to increase the Pt mass fraction to 10 wt.% with the OX-PTA pair, this impregnation-drying-reduction cycle was repeated using the same original catalyst batch: after one cycle, the sample was re-impregnated with 3 mL of PTA solution, then dried and reduced again. Finally, two reference samples were prepared by the previous-developed SEA method [14] using CPA and PTA nitrate as precursors on the same supports (CX and OX, respectively).

The catalysts are labeled using the support name, the precursor name and the preparation technique; when the impregnation is performed twice, a "2" is added at the end of the catalyst name (Table 1). For instance, OX-PTA-CEDI is prepared by the CEDI method with the OX-PTA pair, while OX-PTA-CEDI-2 represents the catalyst obtained by double-impregnation with the same method.

2.3. Catalyst characterization

Scanning Transmission Electron Microscopy (STEM) images were obtained on a JEM-2010F manufactured by JEOL (USA). The particle size distribution of the synthesized catalysts was calculated using the PARTICULE2 software. High angle annular dark field (HAADF) imaging, or "Z contrast" imaging, was performed at 200 kV.

X-ray Diffraction (XRD) analysis was performed on a Siemens D5000 diffractometer with CuK_α radiation operating at 30 kV and 40 mA. The 2θ angle extended from 30° to 60° and varied using a step size of 0.02° accumulating data for 4 s.

In order to detect modifications of the precursor-support interactions, Temperature Programmed Reduction (TPR) was performed on the dried, unreduced samples in an AutoChem II 2920 using a TCD detector. During TPR measurement, the sample was reduced in 10% H_2/N_2 (0.04 mmol min^{-1}) at a heating rate of 10 K min^{-1} from 300 K to 1070 K.

The electrochemically active Pt surface area and the eventual presence of large Pt particles or Pt agglomerates was investigated by CO_{ad} stripping measurements [19,20]. Their electrocatalytic activity for the oxygen reduction reaction (ORR) was investigated in a custom-made four-electrode electrochemical cell using a rotating disk electrode (EDT101, Tacussel) and an Autolab-PGSTA20 potentiostat. The counter-electrode was a large-area Pt foil and the reference electrode was a saturated calomel electrode (SCE: +0.245 V *vs.* the normal hydrogen electrode, NHE) connected to the cell *via* a Luggin capillary. However, all electrode potentials are referred to the normal hydrogen electrode (*i.e.* in V *vs.* NHE). A thin active layer (AL) of Pt/C catalyst was deposited onto a glassy carbon electrode. This electrode (diameter = 5 mm) had been previously polished with diamond paste down to 1 μm and washed for 15 min in three successive ultrasonic baths of acetone, ethanol–water (1:1) and water. The AL was prepared from a suspension blended from a certain amount of catalyst (20 mg of carbon support), 466 mg of 5 wt.% Nafion® in alcohol (Aldrich), and 1.5 mL ultrapure water (18.2 MΩ cm – 3 ppb total organic compounds, Millipore Elix + Gradient). After homogenization in an ultrasonic bath for 1 h, 10 μL of the suspension was deposited onto the electrode and then dried and sintered at 423 K in air. In order to remove the air contained in the AL and to fill its porosity with electrolyte solution, a drop of 1 M H_2SO_4 was deposited onto the catalyst, prior to outgassing under primary vacuum until no air bubbles were visible. All the experiments were carried out in 1 M sulphuric acid (Suprapur-Merck) at 298 K.

In CO_{ad} stripping experiments, the CO saturation coverage was established by bubbling CO for 6 min and purging with Ar for 39 min, while keeping the electrode potential at E = 0.095 V *vs.* NHE. Three voltammetric cycles were then recorded at 0.02 V s^{-1} between +0.05 and +1.23 V *vs.* NHE. The third cycle was subtracted to the first one, and the specific surface area, $S_{CO\text{-}strip}$, was calculated from the charge required to electrooxidize the CO_{ad} monolayer assuming that the electrooxidation of a CO_{ad} monolayer requires 420×10^{-6} C cm_{Pt}^{-2} [21].

The intrinsic ORR activity of the synthesized catalyst was measured in O_2-saturated 1 M H_2SO_4 solution (20 min of purging by oxygen > 99.99%, Messer) by linearly sweeping the potential from 0.40 to 1.00 V *vs.* NHE at a scan rate of 1 mV s^{-1}. The revolution rate was controlled using a MSRX speed controller, and the experiment was repeated at four RDE revolution rates (42, 94, 168 and 262 rad s^{-1}) to account for the diffusion-convection of the reactants in the liquid layer. The intrinsic ORR specific activity was determined at E = 0.85 or 0.90 V *vs.* NHE by normalizing the current measured after correction from the oxygen diffusion in the solution to the real surface area determined by CO_{ad} stripping voltammetry [22]. Note that, prior to the ORR kinetics measurements, the electrodes were cycled between 0.05 and 1.23 V *vs.* NHE at a scan rate of 0.05 V s^{-1} under Ar until reproducible cyclic voltammograms were measured.

3. Results and discussion

The Pt particles obtained *via* different synthesis routes were examined by scanning transmission electron microscopy (STEM). Fig. 3a shows that sample CX-CPA-SEA, obtained by the classical SEA method with the non-oxidized carbon xerogel as support and CPA as precursor feature narrow particle size distribution (standard deviation σ_{TEM} = 0.2, see Table 1) centred on d_{TEM} = 1.5 nm. A similar

Table 1
Platinum mass fraction, mean particle size and ORR kinetics parameters.

Sample	Method	Mass fraction (wt.%) ± 0.1	d_{TEM} (nm)	σ_{TEM} (nm)	$S_{CO\text{-}strip}$ ($m^2\ g_{Pt}^{-1}$) ±10%	b ($V\ dec^{-1}$) ±5%	SA_{85} ($\mu A\ cm_{Pt}^{-2}$) ±5%	SA_{90} ($\mu A\ cm_{Pt}^{-2}$) ±5%
CX-CPA-SEA	SEA	8.5[a]	1.5	0.2	84	−0.068	72	18
OX-PTA-SEA	SEA	4.5[a]	1.6	0.2	119	–[b]	–[b]	–[b]
CX-CPA-CEDI	CEDI	10.0	2.0	0.2	77	−0.073	71	17
OX-PTA-CEDI	CEDI	5.0	1.7	0.2	114	–[b]	–[b]	–[b]
OX-PTA-CEDI-2	CEDI	10.0	1.7	0.2	122	−0.071	65	17

[a] Measured by ICP-AES.
[b] Not measured because of low Pt loading.

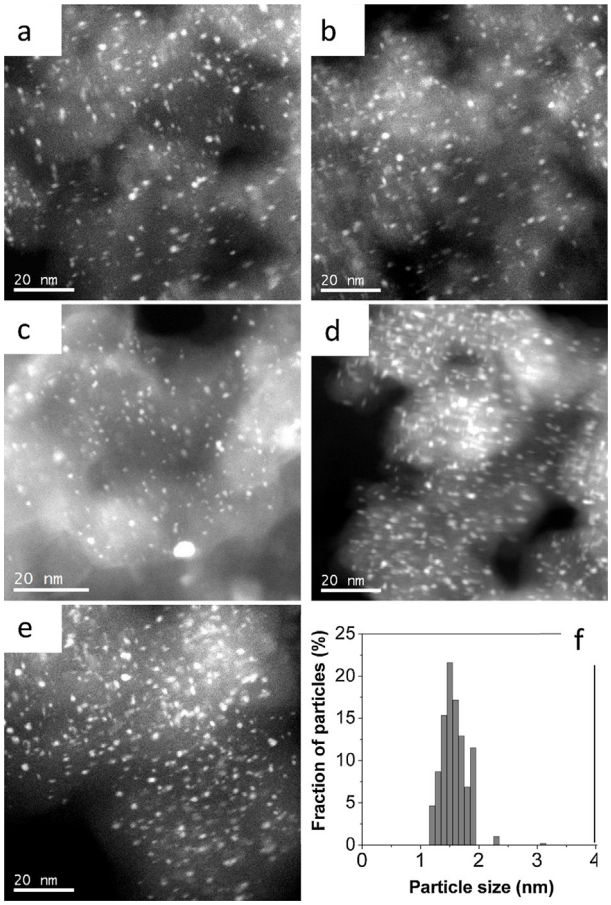

Fig. 3. STEM micrographs and image analysis: (a) CX-CPA-SEA, (b) OX-PTA-SEA, (c) CX-CPA-CEDI, (d) OX-PTA-CEDI, (e) OX-PTA-CEDI-2, and (f) particle size distribution of OX-PTA-CEDI-2.

result was obtained using the SEA method with the OX-CPA pair (Fig. 3b and Table 1), in agreement with our previous work [14]. Fig. 3c and d displays images obtained with the CEDI method applied either to the CX-CPA or to the OX-PTA pair: the results show that the Pt particles deposited over both supports remain small in size (d_{TEM} = 2.0 and 1.7 nm, respectively). Interestingly, similar observations were made from the sample OX-PTA-CEDI-2, which was prepared by double CEDI (Fig. 3(d and e) and Table 1). Whatever the preparation method and the support-precursor pair, the particle size distribution is very narrow (see the values of the standard deviation, σ_{TEM}, in Table 1). As an example, the particle size distribution of sample OX-PTA-CEDI-2 is shown in Fig. 3f; the size distributions obtained with the other samples (not shown) are almost superimposed with this curve.

These results indicate that the CEDI procedure is quite equivalent to the SEA method in terms of obtained metal dispersion. One can thus imagine that the adsorption mechanism remains similar in both techniques, and that the only difference between both deposition techniques is the removal of the Pt solution excess from the system. Another interesting observation lies in the fact that, in the case of the OX-PTA pair, no increase of the particle size is observed after the second impregnation-drying-reduction cycle. This leads to the conclusion that the adsorption sites that have interacted with $[Pt(NH_3)_4]^{2+}$ during the first CEDI procedure were regenerated when the Pt complex was reduced into metallic nanoparticles. The electrostatic interactions between the Pt precursor and the carbon support, which are at the basis of the SEA technique, remain identical in the CEDI method and prevent from Pt agglomeration. It is worth noting that even the reduction treatment does not seem to modify the capability of the carbon support to adsorb $[Pt(NH_3)_4]^{2+}$ cations, which would mean that the oxygen surface groups remaining on the support after oxidation in nitric acid and thermal treatment are not affected by the metal deposition and reduction steps.

The homogenous Pt dispersion observed locally by STEM is confirmed at a larger scale using X-ray diffraction (XRD). Fig. 4

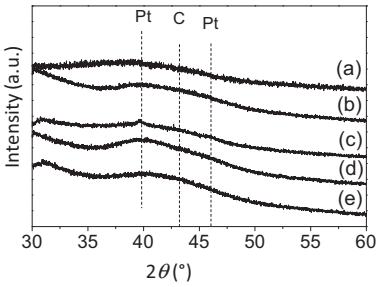

Fig. 4. XRD diffractograms: (a) CX-CPA-SEA, (b) OX-PTA-SEA, (c) CX-CPA-CEDI, (d) OX-PTA-CEDI, and (e) OX-PTA-CEDI-2. The vertical lines indicate the position of the (1 1 1) and (2 0 0) diffraction peaks of Pt nanocrystallites ($2\theta = 39.9^\circ$ and 46.3°) and the two-dimensional lattice reflection of the carbon support ($2\theta = 43.2^\circ$).

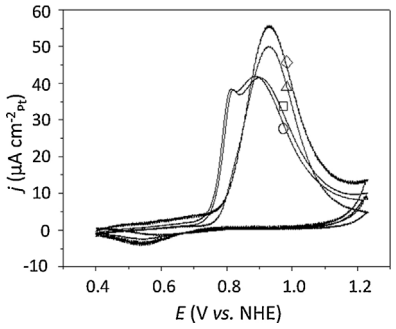

Fig. 6. Background subtracted CO_{ad} stripping voltammogram on the catalysts in 1 M H_2SO_4 at 298 K; sweep rate of 0.020 V s^{-1}. (□) CX-CPA-SEA, (○) CX-CPA-CEDI, (◊) OX-PTA-CEDI, (△) OX-PTA-CEDI-2.

shows XRD patterns of the five Pt/C catalysts. No sharp peaks corresponding to Pt crystals are observed, which confirms that the Pt nanocrystallites are very small in size when either the SEA or the CEDI (simple or double) preparation technique is used with both support-precursor pairs (CX-CPA and OX-PTA).

The Pt dispersion and the Pt particle size distribution largely depend on the strength of interaction between the Pt precursor complex and the carbon support. This parameter was characterized on the unoxidized and oxidized carbon supports by Temperature-Programmed Reduction (TPR) measurements before the reduction treatment. Strong interactions between the adsorbed Pt species and the carbon support, such as those resulting from the SEA preparation technique, make the Pt precursor more difficult to reduce [23], and translate in TPR by a shift toward higher temperature of the TPR peak corresponding to the reduction of the Pt complex surface species. The TPR profiles of the synthesized catalysts are presented in Fig. 5: they indicate that the Pt/C samples prepared with the same support-precursor pair, but using either the SEA or the CEDI method, behave exactly the same; as a conclusion, the strength of the Pt complex-carbon interaction is similar, whatever the impregnation technique, which hints at identical nature of the interactions in SEA and CEDI when the same support-complex pair and pH conditions are used. These interactions remain strong enough to avoid Pt sintering during reduction at 523 K, and lead to high dispersion of Pt.

Fig. 6 shows representative background-subtracted CO_{ad} stripping voltammograms obtained on the four catalysts. The currents are normalized to the real surface area estimated from CO_{ad} stripping coulometry (see experimental), *i.e.* they are expressed in $\mu A\,cm_{Pt}^{-2}$. The curve corresponding to sample OX-PTA-SEA superposes with that of sample OX-PTA-CEDI, and was omitted for clarity. The calculated values of the electrochemically active Pt surface areas, $S_{CO\text{-}strip}$, are reported in Table 1. Fig. 6 clearly shows that the synthesis technique does not influence the results. Indeed,

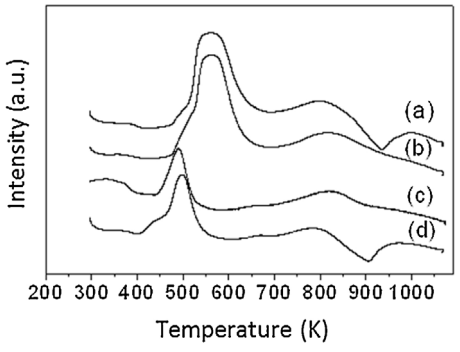

Fig. 5. TPR spectra of samples (a) OX-PTA-SEA, (b) OX-PTA-CEDI-2, (c) CX-CPA-SEA, and (d) CX-CPA-CEDI.

the shape of the voltammograms corresponding to samples CX-CPA-SEA and CX-CPA-CEDI is identical. Both curves display a main electrooxidation peak located at around 0.91 V *vs.* NHE, corresponding to CO oxidation on small particles (<3 nm) [24], while a second peak of much lower intensity, usually ascribed to CO_{ad} electrooxidation on Pt particles larger than 3 nm, appears at lower potential (~0.82 V *vs.* NHE). This pre-peak is not always observed: in previous studies concerning SEA impregnation with CPA, CO_{ad} stripping curves displayed only the main electrooxidation peak corresponding to particles smaller than 3 nm [13,25]. The Pt specific surface area calculated from the coulometry equals 84 and 77 $m^2\,g_{Pt}^{-1}$ for CX-CPA-SEA and CX-CPA-CEDI, respectively, two values which are not significantly different. Summing up, the electrochemical observations parallel remarkably the analyses derived from electron microscopy: they confirm that the synthesized catalysts are identical in terms of metal dispersion and Pt nanostructure. Regarding samples prepared with the OX-PTA pair, one observes that the background-subtracted CO_{ad} stripping voltammograms of samples OX-PTA-CEDI and OX-PTA-CEDI-2 display one single peak whose maximum is located at 0.93 V *vs.* NHE. No pre-peak corresponding to large Pt particles is observed. The Pt specific surface area ranges from 114 to 122 $m^2\,g_{Pt}^{-1}$ (Table 1), two values which are of the same order of magnitude. Again, since no modification is observed, one can conclude that the impregnation procedure (SEA or CEDI) does not affect the morphology of the final catalyst. Similar CO_{ad} stripping curves are also measured depending whether one or two consecutive impregnation-drying-reduction cycles were performed (OX-PTA-CEDI and OX-PTA-CEDI-2 sample): this result strongly support our former assumption that new Pt nanoparticles of the same size were generated during the second cycle.

When comparing the overall results obtained with the five catalysts, one can note that the Pt specific surface areas calculated from the CO_{ad} stripping results, $S_{CO\text{-}strip}$, are lower for the CPA-CX pair (77 and 84 $m^2\,g_{Pt}^{-1}$) than in the case of the PTA-OX pair (114 – 122 $m^2\,g_{Pt}^{-1}$). On the contrary, the Pt particle size measured by image analysis of the STEM micrographs, d_{TEM}, is similar. Such difference can be rationalized by considering that different metal precursors were used in each case: in the case of CPA, both CX-CPA-SEA and CX-CPA-CEDI still contain chlorine species that partly contaminate the Pt surface, and cannot be removed by a single CO_{ad} stripping experiment. Indeed, it has been previously shown that, after reduction at 473 K, Cl adsorbed at the carbon surface, and issued from the decomposition of $PtCl_6^{2-}$, is not completely removed by reduction under hydrogen, even for temperatures as high as 723 K [25]. As a result, some Cl may remain at the Pt particle surface and partly block the electroactive sites, leading to a Pt electroactive surface lower than what is expected from electron microscopy measurements (~120 $m^2\,g_{Pt}^{-1}$ for particle size distributions centred at 2 nm). On the contrary, in the case of PTA, $S_{CO\text{-}strip}$ values of

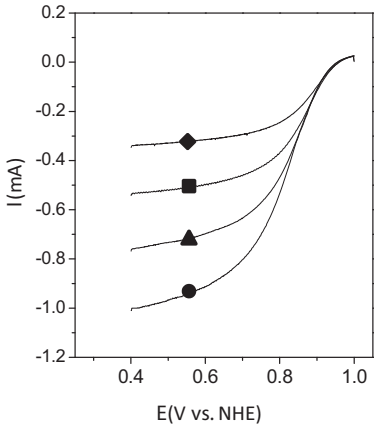

Fig. 7. Example of ORR measurements in O_2-saturated 1 M H_2SO_4 at 298 K, potential sweep rate of 0.001 V s^{-1}, revolution rate of (♦) 62 rad s^{-1}, (■) 94 rad s^{-1}, (●) 168 rad s^{-1} and (▲) 262 rad s^{-1}. Sample CX-CPA-CEDI.

samples OX-PTA-SEA, OX-PTA-CEDI and OX-PTA-CEDI-2 are nearly identical and agree reasonably well with the values determined by transmission electron microscopy (114 – 122 $m^2\ g_{Pt}^{-1}$), which implies that the catalytic surface is "chemically clean".

The ORR activity of the different electrocatalysts was compared with electrodes presenting identical Pt loading and thicknesses. Indeed, the thickness of the catalytic layer, the Pt coverage and the distance between Pt nanoparticles strongly influence the ORR kinetics through transport and re-adsorption effects [26]. The measurements of the ORR kinetics were performed on samples CX-CPA-SEA (Pt mass fraction = 8.5 wt.%), CX-CPA-CEDI (10.0 wt.%) and OX-PTA-CEDI-2 (10.0 wt.%). Fig. 7 shows an example (sample CX-CPA-CEDI) of ORR measurements in O_2-saturated H_2SO_4 solution (1 M) for the four different revolution rates chosen. To evaluate the ORR activity of the three catalysts (CX-CPA-SEA (Pt mass fraction = 8.5 wt.%), CX-CPA-CEDI (10.0 wt.%) and OX-PTA-CEDI-2 (10.0 wt.%)), three parameters were isolated from the ORR measurements: (i) the Tafel slope, *b*, (ii) the specific activity at 0.85 V *vs.* NHE, SA_{85}, and (iii) the specific activity at 0.90 V *vs.* NHE, SA_{90}. These potentials roughly translate to those of a PEMFC cathode operated at low current density (*i.e.* under kinetic control). The results are gathered in Table 1 and are very similar for the three catalysts: the Tafel slope, *b*, ranges from 68 to 73 V dec^{-1}, while values of SA_{85} and SA_{90} range from 65 to 72 μA cm_{Pt}^{-2} and from 17 to 18 μA cm_{Pt}^{-2}, respectively. As a conclusion, no significant difference can be observed between the samples, whatever the precursor-support pair (CPA-CX or PTA-OX) or the impregnation technique (SEA, CEDI or double CEDI).

4. Conclusions

In summary, the 'Charge Enhanced Dry Impregnation' consists in combining the classical dry impregnation technique with the Strong Electrostatic Adsorption method: the support is impregnated with the amount of precursor solution just necessary to fill its porosity, while adjusting the metal content of the solution and its pH to the optimal values deduced from SEA. Compared to the SEA method, the CEDI technique allows obtaining highly dispersed Pt/carbon xerogel catalysts with relatively high Pt mass fraction without any noble metal loss. Owing to the strong electrostatic interactions that exist between the Pt precursor and the carbon support, sintering and agglomeration are prevented during the preparation process so that well-dispersed Pt particles are obtained after reduction.

The Pt specific surface area of the synthesized catalysts does not depend on the impregnation technique used, but is lower in the case of catalysts prepared by SEA or CEDI impregnation of support with a Cl-containing precursor; this result was rationalized on the basis of the blockage of some catalytic sites by Cl atoms or Cl^- ions remaining at the Pt particle surface. Finally, the ORR kinetics measured on the electrocatalysts prepared either by SEA or CEDI (simple or double) and with H_2PtCl_6 or $[Pt(NH_3)_4](NO_3)_2$ is nearly identical: thus, the use of CEDI to replace the metal precursor- and time-consuming SEA technique leads to Pt/C electrocatalysts with adequate properties for fuel cell applications.

This work demonstrates the possibility to use the CEDI method to prepare carbon-supported metal catalysts in many other research areas. Future work will aim at defining the maximum Pt mass fraction that can be achieved on carbon xerogels without altering the metal dispersion or the intrinsic catalytic properties through the use of consecutive CEDI procedures.

Acknowledgements

C.C. thanks the F.R.S.-FNRS (Belgium) for a postdoctoral fellowship grant. G.Y. acknowledges the funding from the Fundamental Research Funds for the Central Universities in China. The Belgian authors also thank the Fonds de Recherche Fondamentale Collective (FRFC no. 2.4.542.10.F), the Ministère de la Région Wallonne (project INNOPEM no. 1117490), the Fonds de Bay and the Interuniversity Attraction Pole (IAP-P6/17) for their financial support.

References

[1] M.S. Dresselhaus, I.L. Thomas, Nature 414 (2001) 332–337.
[2] P. Costamagna, S. Srinivasan, J. Power Sources 102 (2001) 242–252.
[3] K. Sopian, W.R. Wan Daud, Renew. Energy 31 (2006) 719–727.
[4] E. Billy, F. Maillard, A. Morin, L. Guétaz, F. Emieux, C. Thurier, P. Doppelt, S. Donet, S. Mailley, J. Power Sources 195 (2010) 2737–2746.
[5] K. Kinoshita, J. Electrochem. Soc. 137 (1990) 845–848.
[6] X. Yu, S. Ye, J. Power Sources 172 (2007) 133–144.
[7] N.P. Brandon, S. Skinner, B.C.H. Steele, Annu. Rev. Mater. Res. 33 (2003) 183–213.
[8] M. Chisaka, H. Daiguji, Electrochim. Acta 51 (2006) 4828–4833.
[9] C. Bianchini, P.K. Shen, Chem. Rev. 109 (2009) 4183–4206.
[10] E. Antolini, Appl. Catal. B 88 (2009) 1–24.
[11] N. Job, J. Marie, S. Lambert, S. Berthon-Fabry, P. Achard, Energy Convers. Manage. 49 (2008) 2461–2470.
[12] C. Arbizzani, S. Beninati, E. Manferrari, F. Soavi, M. Mastragostino, J. Power Sources 172 (2007) 578–586.
[13] N. Job, S. Lambert, M. Chatenet, C.J. Gommes, F. Maillard, S. Berthon-Fabry, J.R. Regalbuto, J.-P. Pirard, Catal. Today 150 (2010) 119–127.
[14] S. Lambert, N. Job, L. D'Souza, M.F.R. Pereira, R. Pirard, B. Heinrich, J.L. Figueiredo, J.-P. Pirard, J.R. Regalbuto, J. Catal. 261 (2009) 23–33.
[15] J.R. Regalbuto (Ed.), Catalyst Preparation: Science and Engineering, CRC Press, Taylor & Francis Group, Boca Raton, 2007, p. 297.
[16] J.R. Regalbuto, A. Navada, S. Shadid, M.L. Bricker, Q. Chen, J. Catal. 184 (1999) 335–348.
[17] X. Zhu, H.-R. Cho, M. Pasupong, J.R. Regalbuto, ACS Catal. 3 (2013) 625–630.
[18] N. Job, A. Théry, R. Pirard, J. Marien, L. Kocon, J.-N. Rouzaud, F. Béguin, J.-P. Pirard, Carbon 43 (2005) 2481–2494.
[19] F. Maillard, S. Schreier, M. Hanzlik, E.R. Savinova, S. Weinkauf, U. Stimming, Phys. Chem. Chem. Phys. 7 (2005) 385–393.
[20] F. Maillard, E.R. Savinova, U. Stimming, J. Electroanal. Chem. 599 (2007) 221–232.
[21] S. Trasatti, J. Electroanal. Chem. 327 (1992) 353–376.
[22] A.J. Bard, L.R. Faulkner, Electrochemical Methods: Fundamentals and Applications, Wiley, New York, 1992, pp. 283.
[23] L. Jiao, J.R. Regalbuto, J. Catal. 260 (2008) 342–350.
[24] F. Maillard, M. Eikerling, O.V. Cherstiouk, S. Schreier, E. Savinova, U. Stimming, Faraday Discuss. 125 (2004) 357–377.
[25] N. Job, M. Chatenet, S. Berthon-Fabry, S. Hermans, F. Maillard, J. Power Sources 240 (2013) 294–305.
[26] F. Maillard, S. Pronkin, E.R. Savinova, in: W. Vliestich, H. Yokokawa, H.A. Gasteiger (Eds.), Handbook of fuel cells – Fundamentals, Technology and Applications, vol. 5, John Wiley & Sons Ltd., 2009, p. 101.